Influence of the chest compression measurement method on assessment of restraint performance in side-impact Crash Scenarios

Donata Gierczycka, Duane Cronin

PII: S0021-9290(18)30345-2
DOI: https://doi.org/10.1016/j.jbiomech.2018.04.044
Reference: BM 8691

To appear in: *Journal of Biomechanics*

Accepted Date: 25 April 2018

Please cite this article as: D. Gierczycka, D. Cronin, Influence of the chest compression measurement method on assessment of restraint performance in side-impact Crash Scenarios, *Journal of Biomechanics* (2018), doi: https://doi.org/10.1016/j.jbiomech.2018.04.044

An original article

Influence of the Chest Compression Measurement Method on Assessment of Restraint Performance in Side-impact Crash Scenarios

Donata Gierczycka[1], Duane Cronin[1]

[1] University of Waterloo, Waterloo, ON, Canada

Submitted to Journal of Biomechanics

February 9, 2018

Corresponding Author: Duane Cronin, Ph.D.
University of Waterloo
200 University Avenue West
Waterloo, ON, N2L 3G1, Canada
Email: duane.cronin@uwaterloo.ca
Phone: 519-888-4567 x32682
Fax: 519-885-5862

Word Count: Abstract: 249
Introduction – Discussion: 2,559

Keywords: human body model, injury biomechanics, finite element method, side impacts, passive restraints

Abstract

Side impact crashes contribute a significant number of fatal injuries (25% of road fatalities in the USA in 2016), with severe thoracic injuries diagnosed in 58% of front near-side impact occupants. Epidemiological data indicate that thoracic-only side airbags (tSABs) are not as effective as laboratory testing has suggested, and one of the reasons for this may be the use of surrogate-specific injury assessment methods, which are not directly transferable between Anthropometric Test Devices (ATDs) and Post-Mortem Human Surrogates (PMHSs). This study examines the effect of the thorax deformation measurement location and method on the predicted performance of seatbelts and tSABs in a side impact using a Human Body Model (HBM). The HBM was integrated in a vehicle and subjected to a Moving Deformable Barrier (MDB) impact at 61 km/h, with four restraint configurations: belted and unbelted, with and without a tSAB. Occupant response was assessed through chest band (CB) deformation, and as a change in distance between markers on the ribs. Multiple measurement locations in the HBM enabled direct comparison between the methods. The CB method indicated a 35% increase of chest compression due to tSAB; the rib-deflection (RD) method was not sensitive to the tSAB. The RD method predicted a 20% reduction of chest compression due to the seatbelt, but the CB-measured change was negligible. This study highlights the importance of measurement method on the response outcome and demonstrates that different outcomes may be predicted using a HBM for the same impact scenario, depending on the measurement method.

1. Introduction

Side impacts accounted for 5,866 (25)% of the 23,793 passenger vehicle fatalities in the USA in 2016 (IIHS, 2017), and were estimated to be 2.26 times more likely to result in fatal injury compared to frontal impacts, based on the Fatal Accident Reporting System (FARS) data from 1975 to 1998 (Bedard et al., 2002). Countermeasures have been implemented to mitigate injury severity in side impacts, with a focus on padding and airbags to reduce the relative velocity between the occupant and the intruding vehicle door (Strother et al., 1984). Epidemiological data on side-airbag effectiveness have demonstrated a significant reduction in side-impact fatalities, which is attributed to side-curtain and head-and-torso side airbags (D'Elia et al., 2013; Kahane, 2014). The effectiveness of thoracic-only side airbags (tSABs) has not been consistently demonstrated, however (Kahane, 2014; Gaylor and Junge, 2015; Viano and Parenteau, 2016). To further enhance the performance of side restraints, it is necessary to understand the factors contributing to observed differences between laboratory tests and epidemiological data pertaining to occupant response and the potential for injury. Previous studies demonstrated the influence of lateral loading type (Gierczycka et al., 2015a) and occupant pre-crash arm position (Gierczycka et al., 2015b), combined with different restraint configurations (Gierczycka and Cronin, 2017), on the predicted response. However, one important aspect that has been identified (Gierczycka and Cronin, 2017) but not yet addressed is the efficacy of two different methods of quantifying occupant thorax response and predicting the potential for injury.

In Post-Mortem Human Surrogate (PMHS) testing, the response is evaluated using the chest-band (CB) method, whereby the pattern and magnitude of chest deformation, measured as full-chest deflection, is collected via a band with markers placed externally around the PMHS chest at two locations aligned with subject-specific anatomical landmarks, at the level of ribs 8 and 10 (Pintar, 1997). In the Anthropometric Test Devices (ATDs), the rib-deflection (RD) response is measured between two points using a potentiometer at three evenly spaced, discrete locations corresponding to the ATD ribs (FMVSS 214). ATD RD is referred to as the half-chest deflection, and the maximum of three half-chest deflections is converted to the risk of thoracic injury of certain severity (FMVSS 214). Normalized chest compression of 33.9% corresponds to a 50% probability of AIS 3+ (serious, severe, critical or fatal) injury to the thorax (Viano et al., 1989).

Physical experiments have been performed using ATDs and PMHSs. The biofidelity of side-impact ATD responses has been verified through comparison to impactor displacements and accelerations measured in PMHS pendulum impact tests. Comparison of plate forces in rigid-wall sled impact scenarios and accelerations of two thoracic vertebrae measured in PMHS (Ratingen, 2001; Wismans et al., 2005) further contrasted ATD to PMHS response. Therefore, comparison between the ATD and PMHS responses for the ATD development has been based on external kinematic metrics (Pintar, 1997; Kuppa, 2004; Kim, 2016). In order to compare internal, chest-deflection measurements between ATDs and PMHSs, Kuppa et al. (2004) performed 38 PMHS and side-impact ATD rigid-wall sled tests. PMHS half-thorax deflection was measured using chest-bands, while ATD half-thorax deflection was measured using RD potentiometers. Chest-deflection values predicted by the ATD were significantly lower than the PMHS responses, indicating underestimation of the probability of injury to human body with the ATD in Kuppa’s experiment (2004).

Yoganandan et al. (2011) compared the side-impact ATD RD potentiometer measurements to CB-deflection measurements made on the same ATD. The upper CB was located at the level of rib 4 on the ATD, and the lower CB was located at the superior half of the

ATD abdomen. While purely lateral impact responses between the RD and CB methods were comparable within a 5% margin, for oblique impacts the differences between the two were in the order of 300%, which was attributed to padding on the ATD rib modules and jacket (Yoganandan, 2011). Researchers agreed that direct comparison of the side-impact ATD and PMHS responses in impact positions other than purely lateral impacts is challenging, and suggested that additional studies would be needed to quantify the effect of these differences (Ratingen, 2001; Yoganandan, 2011; Wismans, 2005; Cronin, 2011; Kim, 2016; Gierczycka and Cronin, 2017).

This study utilized a detailed, full body HBM, coupled with a restraint system and a full vehicle model, impacted by a Moving Deformable Barrier (MDB) (Fig. 1(a)), and validated against physical test data (Watson, 2011). Thorax responses were measured using a PMHS-specific method (CB method), and an ATD-specific method (RD method). Importantly, measurements could be taken at multiple locations on the thorax, beyond the standard discrete locations. Responses were compared quantitatively as chest compression values, and qualitatively in terms of chest deformation patterns.

2. Materials and methods

A detailed numerical model of the Ford Taurus 2001 model (Fig. 1(a)) (Opiela, 2008), previously assessed and validated in side impact with respect to NCAP and FMVSS 214 test data (Watson, 2011), was coupled with a detailed numerical HBM, the GHBMC M50-O Version 4.3 (Fig. 1(b)) (GHBMC, 2014), following the methods developed by Gierczycka et al.(2015, 2017).

The simulations were performed using a multi-physics explicit code (LS-Dyna R6.1.1, LSTC Livermore).

The HBM was a detailed anatomical representation of a 50th percentile male (M50), and the model verification and validation was performed at the material level, at body region level and at the full body level, under various loading conditions representative of automotive impacts (GHBMC, 2014). The HBM capacity to predict tissue-level injury, such as rib fractures, was enabled through material models, including failure criteria (GHBMC, 2014). The internal contacts within the HBM were defined as sliding surface-to-surface, tied, tied with offset, or tied with a tie-break criterion, to reflect physical connections and interfaces within the human body (GHBMC 2014). The specific contact treatments were determined and validated through 181 impact scenarios at the body region levels, and 9 cases at the full body level (GHBMC 2014).

To couple the occupant with the vehicle, the HBM was equilibrated with the seat using a pre-simulation with use of the gravity force only, and ensuring no initial penetration between the HBM, the seat and the vehicle interior. The pre-simulation was terminated when the pelvis vertical acceleration reached zero and a standard driving position was established (FMVSS 214). Four combinations of the restraints were modeled (Fig. 2), following the method established in a previous study (Gierczycka and Cronin, 2017), to provide a spectrum of loading.

In the belted configurations, the occupant was restrained with a three-point seatbelt, where 2-D shell elements were used for seatbelt segments contacting the HBM, and 1-D beam elements were used outside of the contact region (Baudrit, 1999). The seatbelt model (Watson and Cronin, 2011) included a pre-tensioner and retractor with characteristics based on data from Baudrit et al. (1999). For configurations -B+tSAB and +B+tSAB, a tSAB model was fitted on the vehicle door, to cover the shoulder and upper thorax area and to fill the initial gap between the occupant and door during impact (Gierczycka et al., 2017). The airbag was a simplified rectangular chamber of approximately 6l volume measured during a static deployment test, and reaching pressure of 400 kPa and thickness of 130 mm to match the side restraint criteria established by Haland and Pipkorn (1996). The coupled vehicle-restraint-occupant model was subjected to a MDB impact at 61 km/h (16.9m/s) (NHTSA, 2012) (Fig. 1(a)).

Contacts between the HBM and the vehicle interior, seat, and the restraints, were defined as sliding surface-to-surface penalty-based contacts. The contact penalty stiffness was dependent on the material properties of the parts in contact, namely their stiffness defined at the individual part level, and on the coefficient of friction defined between the parts. The coefficient of static friction for the HBM to vehicle interior contacts was 0.3, typical for the fabric-to-fabric or skin-to-fabric contacts (Vilhena and Ramalho 2016) and comparable to the coefficient of friction of 0.294 measured experimentally between the PMHS and a seat in a lateral impact (Lessley et al. 2010). The dynamic friction of 0.35 reflected the lower range of dynamic coefficients of friction measured for a range of automotive seat covers and occupant clothes (0.344-0.906) (Cummings et al. 2009).

Two measurement methods were used to assess chest compression resulting from the impact: the chest-band (CB) method; and the rib-deflection (RD) method. In the CB method, the chest compression was measured as a change in distance between markers located on the outside of the thorax, at three locations. The upper (rib 8) and lower (rib 10) CB locations corresponded to PMHS CB locations (Pintar, 1997), and a middle CB location (rib 9) was also included in order to provide additional information on the deformation profile of the thorax (Fig. 3(c)). Chest compression measurement for the CB was based on the central thorax deflection methodology described by Shaw (Shaw et al., 2014), and defined as a change in length between the opposing measurement points due to impact deformation, divided by the pre-crash thorax width (Fig. 3(a)).

The RD method assessed chest compression through measurement of change of distance between measurement points directly on the ribs, at the location of maximum rib curvature, and symmetric with respect to the coronal plane (Fig. 3(b)). Measurements were taken on the HBM ribs 4, 6, 8 – which are comparable to locations of the ribs in the ATDs (Gierczycka et al., 2015) – and ribs 9 and 10, to match the CB locations (Fig. 3(c)).

3. Results

The chest compression values predicted for all four restraint configurations were below the threshold of 33.9%. The highest chest compression (27%) was measured at the upper chest band for the unbelted configuration with a tSAB (Table 1).

Table 1
Effect of the restraints on chest deflection for different measurement methods

Compared configurations	Chest-band method	Rib-deflection method
-B-tSAB and +B-tSAB	Seatbelt increased chest compression (largest increase: from 16% to 25%).	Seatbelt had no effect on chest compression.
-B+tSAB and +B+tSAB	Seatbelt had no effect on chest compression.	Seatbelt reduced chest compression (largest reduction: from 24% to 19%).

The RD method demonstrated no change in chest compression values and chest compression pattern between belted and unbelted configurations without the tSAB. In contrast, the CB method demonstrated an increase in chest compression values for the belted occupant, due to the seatbelt loading occurring directly at the measurement location. The maximum chest compression occurred at the lower chest-band level for both belted and unbelted configurations with no tSAB (Fig. 4).

When the tSAB was fitted in the vehicle, the CB compression magnitudes and patterns for the unbelted and belted configurations were comparable. The maximum CB compression was predicted to occur at the upper CB level for both the belted and unbelted configurations with tSAB. In contrast, with the RD method the maximum chest compression for the unbelted occupant was evenly distributed across ribs 4–6, while for the belted occupant the maximum chest compression occurred at the level of ribs 8 and 9 only (Fig. 5).

4. Discussion

The HBM chest band (CB) responses predicted in this study at the upper and lower CB (16% and 21%, respectively) are comparable with the average CB deflections of 13% (CB at the level of rib 8) and 27% (CB at the level of rib 10) measured by Yoganandan and Pintar (1997) in padded flat-wall sled impacts at 6.7 m/s with PMHS. The impact energy transferred to the occupant body during a 6.7 m/s flat-wall sled impact was comparable to the full vehicle side impact at 61 km/h (16.9 m/s) simulated in this study.

The response of the HBM in a rigid-sled impact at 6.7 m/s was previously compared to PMHSs by Hayes et al. (2014). Deformation patterns of the chest bands were comparable between the HBM and three PMHSs at the time of maximum loading. The differences between the peak compressions predicted by the HBM and the PMHSs varied between 6% and 14%, and Hayes (2014) attributed these differences to the model material properties and differences in ribcage geometry between the model and the PMHSs. The HBM peak chest compression values predicted by Hayes et al. (2014) were 28%, 26% and 20% for the upper, middle and lower chest band, respectively. Chest-band compression values reported by Yoganandan and Pintar (1997) were 24% for the CB at the level of rib 8 (upper) and 16% for the CB at the level of rib 10 (lower).

While research on frontal impacts demonstrated advantages of measuring chest deflection at multiple locations rather than at a few discrete locations (Kemper, 2016), there have been very few such investigations for side impacts. This study demonstrated that discrete RD measurement locations at the level of ribs 4–8, corresponding to locations of the side-impact ATD ribs, did not capture the maximum chest compression locations occurring at the level of ribs 9 and10 (Fig. 4(a), 4(b)). Incorporating more measurement locations allowed us to identify the effect of restraint combinations beyond the three discrete locations. For example, while adding the tSAB increased the maximum chest compression values for the unbelted occupant (Fig. 4(a)), it also distributed the load, and therefore the chest compression, evenly over the torso (Fig. 5(a)).

Frontal impact studies have also demonstrated that ATD-based metrics implemented in the HBM were less sensitive to different restraint settings than PMHS-based and tissue level predictions, such as CB deflection and rib strain distribution (Danelson, 2015). The current study verified Danelson’s observation, but for side-impact scenarios, demonstrating increased sensitivity of the ATD-based metrics (RD method) when the tSAB was present, and increased sensitivity of the HBM-based metrics (CB method) when no tSAB was present in the vehicle.

Anthropometric differences between occupants are yet another incentive to include more measurement locations in the injury assessment. In the ATD the ribs are evenly spaced and have the same breadth at all three levels, but in the human thorax the distances between the left and right rib are shorter in the upper thorax (21 cm between apexes of the left and right second rib, measured with the HBM), and greater in the lower thorax (29 cm between left and right eighth rib, measured with the HBM), decreasing again for ribs 9–12. Current side-impact occupant response assessment standards are based on the maximum ATD rib deflection. While for the ATD the location of the maximum rib deflection would not affect the chest compression values, in the human thorax the same magnitude would yield different compression values at different chest levels. Therefore, it is recommended to analyze all the chest deflection locations, preferably collecting data at all the chest levels where the occupant body contacts the restraints and vehicle interior. A comparison of the outcomes of both CB and RD response measurement methods with use of a HBM would provide a better understanding of the restraint and interior design outcomes for occupant safety.

In conclusion, this study demonstrated that two different measurement methods used in biomechanical research yielded different conclusions regarding the effect of vehicle restraint systems configurations on the occupant response. Direct comparison between the CB and RD methods was permitted by application of a detailed finite element HBM in a full vehicle side-impact crash scenario.

Conflict of interest

The authors have no conflict of interest to declare.

Acknowledgements

The authors would like to acknowledge the Global Human Body Model Consortium for use of the HBM, the National Crash Analysis Centre for the vehicle model, the Compute Canada for computational resources, and the Natural Sciences and Engineering Research Council of Canada for funding.

References:

Baudrit, P., Hammon, J., Song, E., Robin, S., Le Coz, J.-Y., 1999. Comparative Studies of Dummy and Human Body Models Behavior in Frontal and Lateral Impact Conditions. Proceedings of the 43rd Stapp Car Crash Conference, 99SC05, San Diego, CA.

Bédard, M., Guyatt, G.H., Stones, M.J., Hirdes. J.P., 2002. The Independent Contribution of Driver, Crash, and Vehicle Characteristics to Driver Fatalities. Accident Analysis and Prevention 34 (6), 717–727.

Cummings, J.R., Osterholt, G.D., Van Calhoun, D., Biller, B.A., 2009. Occupant Friction Coefficients on Various Combinations of Seat and Clothing. SAE Technical Paper Series, No. 2009-01-1672, 1-11. SAE International, Troy, MI.

Danelson, K.A., Golman, A.J., Kemper, A.R., Gayzik, F.S., Gabler, H.C., Duma, S.M., Stitzel, J.D., 2015. Finite Element Comparison of Human and Hybrid III Responses in a Frontal Impact. Accident Analysis and Prevention 85, 125–156.

D'Elia, A., Newstead, S., Scully, J., 2013. Evaluation of Vehicle Side Airbag Effectiveness in Victoria, Australia. Accident Analysis and Prevention 54, 67–72.

Fatal Accident Reporting System, 2016, NHTSA (www-FARS.nhtsa.dot.gov).

Gaylor, L., Junge, M., 2015. Assessment of the Efficacy of Vehicle Side Airbags: A Matched Cohort Study of Vehicle-Vehicle Side Collisions using the GIDAS Database. Proceedings of the IRCOBI Conference, Lyon, France.

Global Human Body Models Consortium (GHBMC), 2014. Available at http://www.ghbmc.com.

Gierczycka, D. and Cronin, D.S., 2015a. Investigation of Human Body Model Response to Different Lateral Loading Conditions. Proceedings of the IRCOBI Conference, Lyon, France.

Gierczycka, D., Watson, B., Cronin, D.S., 2015b. Investigation of Occupant Arm Position and Door Properties on Thorax Kinematics in Side Impact Crash Scenarios-Comparison of ATD and Human Models. International Journal of Crashworthiness 20 (3), 242–269.

Gierczycka, D., Cronin, D.S., 2017. Occupant Thorax Response Variations Due to Arm Position and Restraint Systems in Side Impact Crash Scenarios. Accident Analysis and Prevention 106, 173–180.

Hayes, A.R., Vavalle, N.A., Moreno, D.P., Stitzel, J.D., Gayzik, S.F., 2014. Validation of Simulated Chestband Data in Frontal and Lateral Loading using a Human Body Finite Element Model. Traffic Injury Prevention 15 (2), 181–186.

Insurance Institute of Highway Safety, 2017. 2016 Fatality Facts. Available at http://www.iihs.org/iihs/topics/t/general-statistics/fatalityfacts/overview-of-fatality-facts.

Kahane, C.J., 2014. Updated Estimates of Fatality Reduction by Curtain and Side Air Bags in Side Impacts and Preliminary Analyses of Rollover Curtains. Report no. DOT HS 811 882, National Highway Transport Safety Administration, Washington, DC.

Kemper, A.R., Beeman, S.M., Porta, D.J., Duma, S.M., 2016. Non-censored Rib Fracture Data during Frontal PMHS Sled Tests. Traffic Injury Prevention 17 (S1), 131–140.

Kim, T., Shaw, G., Lessley, D., Park, G., Crandall, J., Svendsen, A., Whitcomb, B., Ayyagari, M., Mishra, P., Markusic, C., 2016. Biofidelity Evaluation of WorldSID and ES-2re under Side Impact Conditions with and without Airbag. Accident Analysis and Prevention 90, 140–151.

Kuppa, S., 2004. Injury Criteria for Side Impact Dummies. National Highway Traffic Safety Administration, Washington, DC.

Lessley D., Shaw, G., Parent, D., Arregui-Dalmases, C., Kindig, M., Riley, P., Pursetzov, S., Sochor, M., Gochenour, T., Bolton, J., Subit, J., Crandall, J., Takayama, S., Ono, K., Kamiji, K., Yasuki, T., 2010. Whole-Body Response to Pure Lateral Impact. Stapp Car Crash Journal 54, paper No. 2010-22-0014, 289-336. The Stapp Association, Ann Arbor, MI.

Mertz, H., Irwin, A.L., Prasad, P., 2003. Biomechanical and scaling bases for frontal and side impact injury assessment values. Stapp Car Crash J. 47, 155–188.

NHTSA, 2006. Laboratory test procedure for FMVSS No. 214 dynamic side impact protection, Document Number TP214D-08 Part 1. National Highway Traffic Safety Administration, Washington, DC.

NHTSA, 2012. Laboratory Test Procedure for the New Car Assessment Program Side Impact Moving Deformable Barrier Test. National Highway Transport Safety Administration, Washington, DC.

Opiela, K.S., 2008. Finite element model of Ford Taurus. NHTSA finite element model archive. Available at http://www.ncac.gwu.edu/vml/archive/ncac/vehicle/taurus-v3.pdf, accessed June 3, 2011.

Pintar, F.A., Yoganandan, N., Hines, M.H., Maltese, M.R., McFadden, J., Saul, R., Eppinger, R., Khaewpong, N., Kleinberger, M., 1997. Chestband Analysis of Human Tolerance to Side Impact. Proceedings of the 41st Stapp Car Crash Conference, 973320, Lake Buena Vista, FL.

Pipkorn, B., Haland, Y., 1996. A Side Airbag System to Meet Chest Injury Measures: Evaluation by Mathematical Simulations. International Journal of Crashworthiness 1 (1), 145-161.

Ratingen, M., 2001, Development and Evaluation of the ES-2 Side Impact Dummy. Proceedings of the 17th Conference on Enhanced Safety of Vehicles, paper No. 336, Amsterdam, Netherlands.

Shaw, G., Lessley, D.J., Ash, J.L., Sochor, M.R., Crandall, J.R., Luzon-Narro, J., Arregui-Dalmases, C., 2014. Side impact PMHS thoracic response with large-volume air bag, Traffic Injury Prevention 15, 40–47.

Strother, C.E., Smith, G.C., James, M.B., Warner, C.Y., 1984. Injury and Intrusion in Side Impacts and Rollovers. SAE Technical Paper Series No. 840403. SAE International, Troy, MI

Viano, D.C., Lau, I.V., Asbury, C., King, A.I., Begeman, P., 1989. Biomechanics of the Human Chest, Abdomen, and Pelvis in Lateral Impact. Accident Analysis and Prevention 21 (6), 553–574.

Viano, D.C., Parenteau, C.S., 2016. Difference in Dummy Responses in Matched Side Impact Tests of Vehicles with and without Side Airbags. Traffic Injury Prevention 17 (5), 524–529.

Vilhena, L., and Ramalho, A., 2016. Friction of Human Skin against Different Fabrics for Medical Use. Lubricants 4 (6), 1-10.

Watson, B., Cronin, D.S., 2011. Side impact occupant response with varying positions. International Journal of Crashworthiness 16 (5), 569–582.

Wismans, J., Happee, R., van Dommelen, J.A.W., 2005. Computational human body models, IUTAM Proceedings on Impact Biomechanics: From Fundamental Insights to Applications, Michael D. Gilchrist, ed., Springer Academic Publishers, Dordrecht, 417–429.

Yoganandan, N., Pintar, F.A., 1997. NHTSA Test Reports: Side Impact Test with Human Surrogate: B3120, B3122, B3155, B3588, B3663, B3664, B3700, B3276, B3277, and B3719. National Highway Transport Safety Administration, Washington, DC.

Yoganandan, N., Humm, J.R., Pintar, F.A., Brasel, K., 2011. Region-Specific Deflection Responses of WorldSID and ES2-re Devices in Pure Lateral and Oblique Side Impacts. Stapp Car Crash Journal, 55, 351–378.

Fig. 1. (a) NCAP MDB-vehicle model with occupant, and (b) HBM integrated with the vehicle and restraints.

Fig. 2. Restraint system configurations for vehicle side-impact scenario.

Fig. 3. Chest compression measurement location: (a) chest-band (CB) method; (b) rib-deflection (RD) method; (c) tissue outer contour with chest-band locations marked with respect to the ribcage.

Fig. 4. Chest compression values for (a) unbelted and (b) belted configurations without the tSAB, measured with RD and CB methods.

Fig. 5. Chest compression values for (a) unbelted and (b) belted configurations with the tSAB, measured with RD and CB methods.

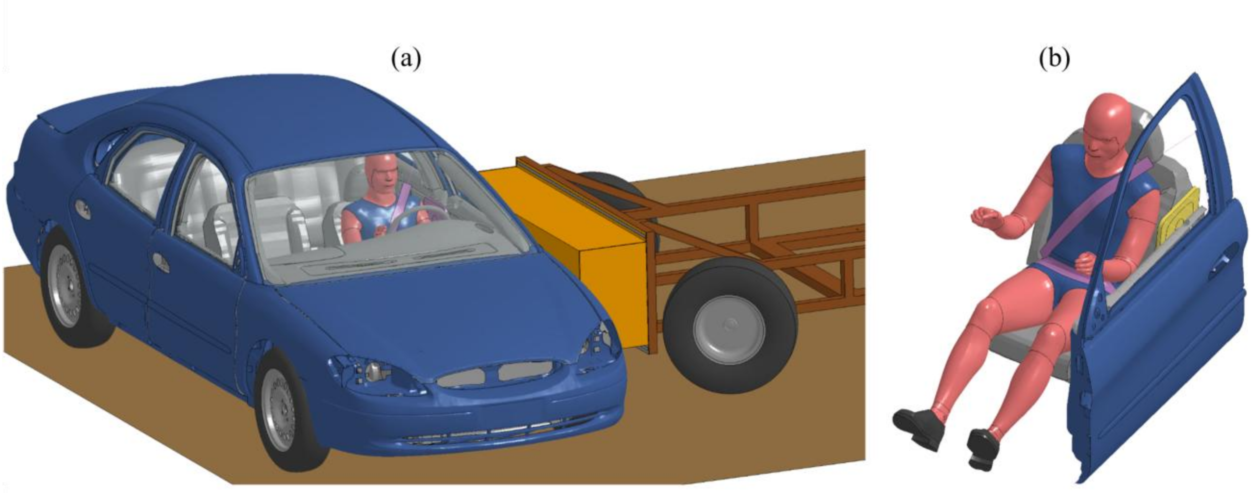
(a)
(b)

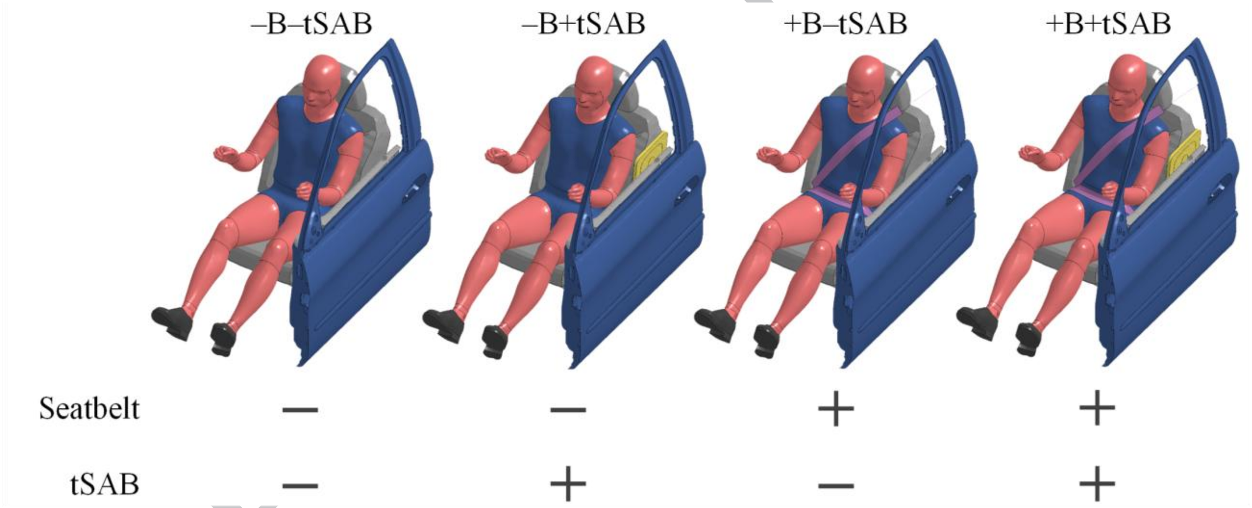
–B–tSAB
–B+tSAB
+B–tSAB
+B+tSAB
Seatbelt
–
–
+
+
tSAB
–
+
–
+

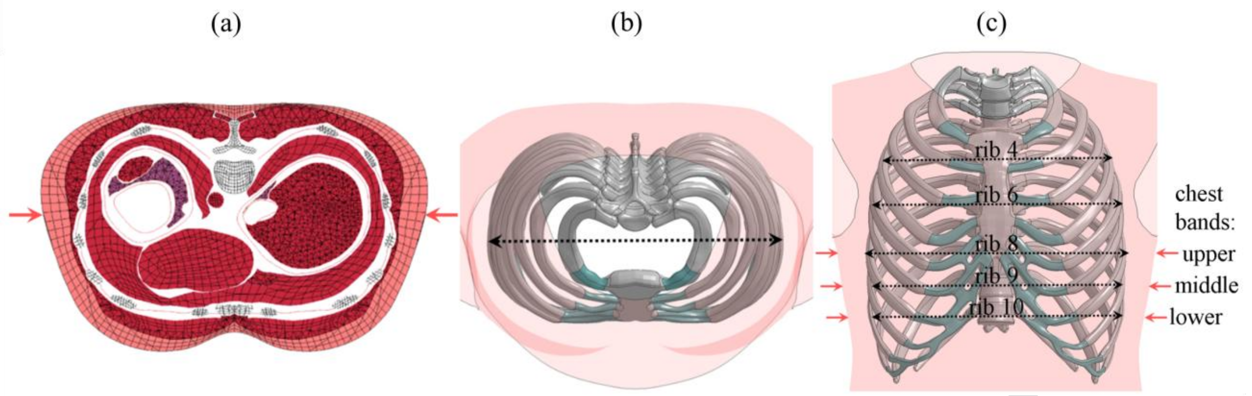
(a)
(b)
(c)
rib 4
rib 6
rib 8
rib 9
rib 10
chest bands:
upper
middle
lower

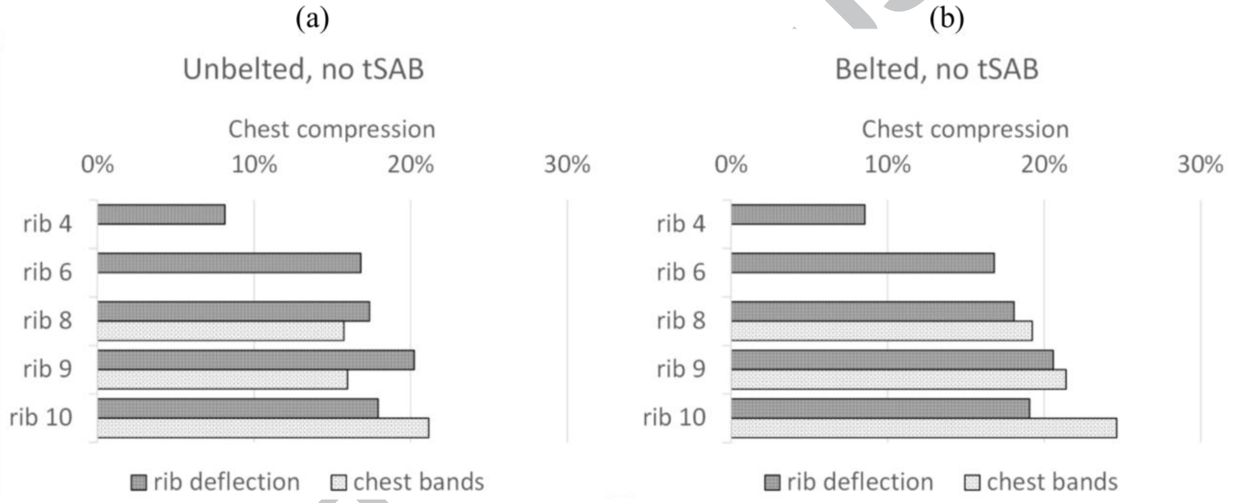
(a)
Unbelted, no tSAB
Chest compression
0%
10%
20%
30%
rib 4
rib 6
rib 8
rib 9
rib 10
rib deflection
chest bands
(b)
Belted, no tSAB
Chest compression
0%
10%
20%
30%
rib 4
rib 6
rib 8
rib 9
rib 10
rib deflection
chest bands

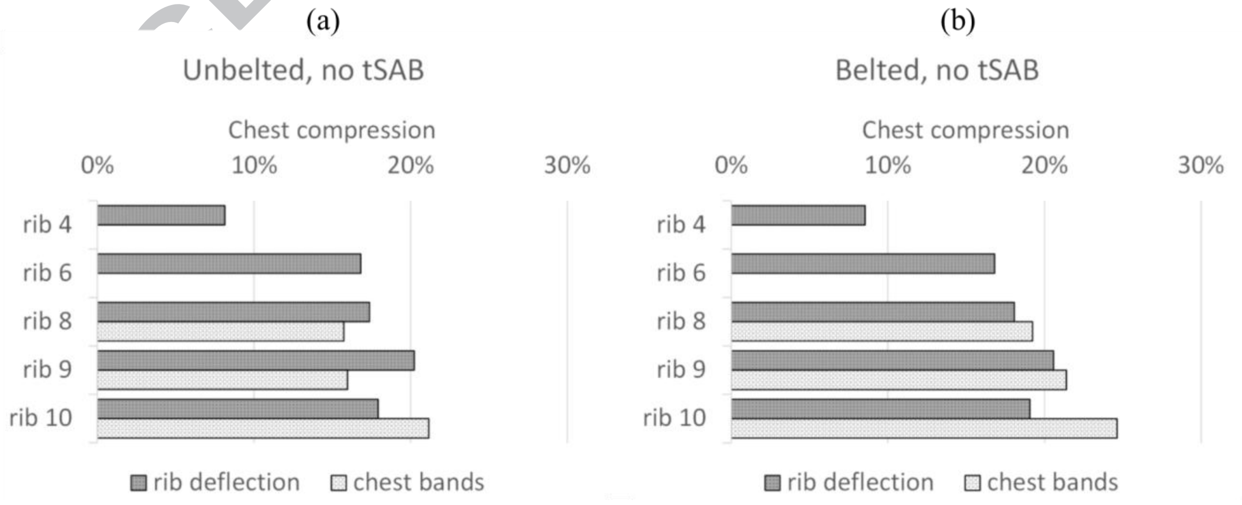
(a)
Unbelted, no tSAB
Chest compression
0%
10%
20%
30%
rib 4
rib 6
rib 8
rib 9
rib 10
rib deflection
chest bands
(b)
Belted, no tSAB
Chest compression
0%
10%
20%
30%
rib 4
rib 6
rib 8
rib 9
rib 10
rib deflection
chest bands